# Pulsed Electromagnetic Field Signal Transfer Across a Thin Magneto-Dielectric Sheet

Štumpf, Martin; Antonini, Giulio ; Lager, Ioan E.; Vandenbosch, Guy A.E.

**DOI**
10.1109/TEMC.2021.3056484

**Publication date**
2021

**Document Version**
Accepted author manuscript

**Published in**
IEEE Transactions on Electromagnetic Compatibility

# Pulsed Electromagnetic Field Signal Transfer Across a Thin Magneto-Dielectric Sheet

Martin Štumpf, *Senior Member, IEEE*, Giulio Antonini, *Senior Member, IEEE*, Ioan E. Lager, *Senior Member, IEEE*, and Guy A. E. Vandenbosch, *Fellow, IEEE*

***Abstract*—Closed-form time-domain (TD) analytical expressions describing the electromagnetic (EM) signal transfer between two vertical dipoles through a thin, highly contrasting layer with combined magneto-dielectric properties are derived via the Cagniard–DeHoop (CdH) technique with the TD saltus-type conditions. The TD EM-field coupling between the antennas in the absence of the layer is discussed, including its near-field asymptotic solution. It is demonstrated both analytically and numerically that under certain circumstances the combined sheet behaves virtually as a transparent sheet the transition across which inverts the polarity of the received signal.**

***Index Terms*—Cagniard–DeHoop (CdH) technique, electromagnetic (EM) interference, Green's functions, pulsed EM field transfer, shielding, time-domain (TD) analysis.**

## I. Introduction

THIN sheets play a conditional role in a number of technologies of rapidly expanding economical significance. The shielding properties of such layers are of relevance for ensuring electromagnetic compatibility (EMC) compliance and in wireless power transfer systems [1]–[4].

The vast majority of works studying the shielding effectiveness of planar sheets are concerned with the corresponding frequency-domain analysis [5]–[8]. To take another step further, this article will address the EM shielding problem by presenting a time-domain (TD) analytical investigation of the on-axis EM signal transfer between two spatially localized, fundamental EM sources separated by a thin highly contrasting layer with combined magnetic and dielectric properties. To that end, we employ the classic Cagniard–DeHoop (CdH) technique [9] and the TD saltus type conditions introduced in [10] (see also [11]). Previous applications of the CdH technique to similar problems were confined to the investigation of thin conductive sheets supporting electric currents, only [12]–[17]. This article presents a conceptual extension by incorporating the magnetic and dielectric properties that account for the effect of both electric and magnetic currents induced in the layer. To the best of authors' knowledge, the study of a pulsed EM signal transfer through such a combined sheet has not been attempted before, the hereby introduced closed-form, TD analytical expressions being entirely new.

The derived analytical expressions and the discussed numerical examples have a clear practical applicability. They will cogently show that, under specific conditions, a combination of layers behaves as a transparent sheet and merely inverts an incoming pulse's polarity. This observation has a twofold direct applicability. 1) It provides a unique instrument for evaluating the EM shielding performance of thin magneto-dielectric sheets directly in the TD [2]. 2) The shielding/reflecting properties of thin layers are central to the functioning of specific radiators that are seen as preferred candidates for ultrafast, low-THz communication scenarios [18].

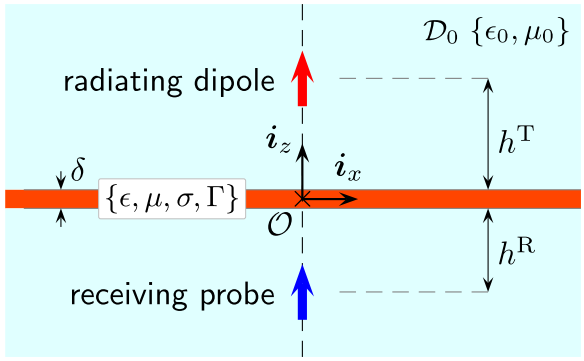


Fig. 1. Problem configuration consisting of transmitting and receiving dipole antennas in the presence of a combined sheet.

## II. Problem Description

The problem configuration under consideration is shown in Fig. 1. Here, the position is specified by the coordinates $\{x, y, z\}$ with respect to the orthogonal Cartesian coordinate system with its origin $\mathcal{O}$ and the standard base $\{\boldsymbol{i}_x, \boldsymbol{i}_y, \boldsymbol{i}_z\}$. Noting the rotational symmetry about the $z$-axis, subscripts $\{r, \phi, z\}$ will

This work was supported by the Czech Science Foundation under Grant 20-01090S. *(Corresponding author: Martin Štumpf.)*

Martin Štumpf is with the Department of Radioelectronics, Faculty of Electrical Engineering and Communication, Brno University of Technology, 61600 Brno, The Czech Republic (e-mail: martin.stumpf@centrum.cz).

Giulio Antonini is with the UAq EMC Laboratory, University of L'Aquila, 67100 L'Aquila, Italy (e-mail: giulio.antonini@univaq.it).

Ioan E. Lager is with the Faculty of Electrical Engineering, Mathematics and Computer Science, Delft University of Technology, 2628 Delft, CD, The Netherlands (e-mail: i.e.lager@tudelft.nl).

Guy A. E. Vandenbosch is with the Department of Electrical Engineering, Division ESAT-TELEMIC (Telecommunications and Microwaves), Katholieke Universiteit Leuven, B-3001 Leuven, Belgium (e-mail: guy.vandenbosch@esat.kuleuven.be).

denote the radial, azimuthal, and axial EM-field components, respectively. The time coordinate is $\{t \in \mathbb{R}; t > 0\}$. Furthermore, the time-convolution operator is denoted by $*_t$, the time differentiation and integration operators are denoted by $\partial_t$ and $\partial_t^{-1}$, respectively, and the Heaviside unit-step function is denoted by $\mathrm{H}(t)$.

The problem configuration consists of transmitting (denoted by $^{\mathrm{T}}$) and receiving (denoted by $^{\mathrm{R}}$) dipole antennas whose dipole moment is oriented along the $z$-direction. We shall analyze the EM interaction between both vertical magnetic and electric dipole antennas that are represented by conducting, relatively small (horizontal) loops (denoted by $\mathcal{L}^{\mathrm{T,R}}$) and short (vertical) wires (denoted by $\mathcal{W}^{\mathrm{T,R}}$), respectively, both carrying the uniform electric current [19, Secs. 26.9 and 26.10]. The transmitting dipole antenna that is located at a height $h^{\mathrm{T}} > 0$ above the layer is at $t = 0$ activated by the (causal) electric current pulse, $I^{\mathrm{T}}(t)$, injected into its port. Its pulse time width is denoted by $t_{\mathrm{w}}$. The main objective of this article is to describe the (open-circuit) voltage pulse, say $V^{\mathrm{R}}(t)$, induced across the port of a receiving probe located at $z = -h^{\mathrm{R}}$ below the combined sheet. The on-axis pulsed EM signal transfer can be represented by $V^{\mathrm{R}}(t) = Z(t) *_t I^{\mathrm{T}}(t)$, where $Z(t)$ is the pertaining transfer impedance. The dipole antennas are separated by a relatively thin, highly contrasting planar sheet with combined magnetic and dielectric properties. The EM properties of the combined layer are described by its (scalar, real-valued, and positive) electric permittivity $\epsilon$, electric conductivity $\sigma$, magnetic permeability $\mu$, and by parameter $\Gamma$ representing linear magnetic hysteresis losses [19, Sec. 26.1]. These parameters are assumed to be relatively high with respect to the electric permittivity, $\epsilon_0$, and magnetic permeability, $\mu_0$, of the homogeneous, isotropic, and loss-free surrounding medium in $\mathcal{D}_0$. The corresponding EM wave speed is $c_0 = (\epsilon_0\mu_0)^{-1/2} > 0$ and the wave admittance is $Y_0 = (\epsilon_0/\mu_0)^{1/2} > 0$.

## III. Problem Formulation

In this section, the desired induced voltage pulse $V^{\mathrm{R}}(t)$ is related to the pertaining EM field. The formulations concerning the TD EM fields radiated from small-loop and short-wire antennas in the presence of a combined sheet are given separately.

### A. Radiating Loop $\mathcal{L}^{\mathrm{T}}$

Assuming the transmitting horizontal loop $\mathcal{L}^{\mathrm{T}}$ above the layer, the nonvanishing tangential EM-field components are the azimuthal component of the electric-field strength $E_\phi$ and the radial component of the magnetic-field strength $H_r$. Referring to Fig. 1, the EM field quantities are rotationally symmetric about the $z$-axis. When crossing the combined layer, they satisfy [10, eqs. (3) and (4)]

$$E_\phi^+ - E_\phi^- = (R^{\mathrm{M}} + L^{\mathrm{M}}\partial_t)\langle H_r\rangle_-^+ + o(\delta) \tag{1}$$

$$H_r^+ - H_r^- = (G^{\mathrm{E}} + C^{\mathrm{E}}\partial_t)\langle E_\phi\rangle_-^+ + o(\delta) \tag{2}$$

for all $r > 0$ and $t > 0$ as $\delta \downarrow 0$, where superscripts $^+$ and $^-$ denote the field values approaching the upper and lower surface of the layer, respectively, and the operator $\langle\rangle_-^+$ has the meaning of arithmetic mean $\langle f\rangle_-^+ = (f^+ + f^-)/2$. Furthermore, the coefficients in (1) and (2) can be viewed as equivalent layer's Kirchhoff's electric-circuit elements [10, eqs. (5) and (6)]

$$G^{\mathrm{E}} = \int_{\zeta=-\delta/2}^{\delta/2} \sigma(\zeta)\mathrm{d}\zeta \text{ and } C^{\mathrm{E}} = \int_{\zeta=-\delta/2}^{\delta/2} \epsilon(\zeta)\mathrm{d}\zeta \tag{3}$$

$$R^{\mathrm{M}} = \int_{\zeta=-\delta/2}^{\delta/2} \Gamma(\zeta)\mathrm{d}\zeta \text{ and } L^{\mathrm{M}} = \int_{\zeta=-\delta/2}^{\delta/2} \mu(\zeta)\mathrm{d}\zeta. \tag{4}$$

The EM contrast of the layer is assumed to be relatively high (with respect to the embedding) such that the coefficients are of $O(1)$ as $\delta \downarrow 0$. Under the assumption that the receiving loop is relatively small, the induced voltage in $\mathcal{L}^{\mathrm{R}}$ can be found from [20, eq. (33)]

$$V^{\mathrm{R}}(t) \simeq -\mu_0\mathcal{A}^{\mathrm{R}}\partial_t H_z(0, -h^{\mathrm{R}}, t) \tag{5}$$

where $\mathcal{A}^{\mathrm{R}}$ is the receiving loop's area and $H_z = H_z(r, z, t)$ denotes the $z$-component of the magnetic-field strength radiated from $\mathcal{L}^{\mathrm{T}}$.

### B. Radiating Wire $\mathcal{W}^{\mathrm{T}}$

If the EM field in the configuration is radiated from the short wire $\mathcal{W}^{\mathrm{T}}$, the nonvanishing tangential EM field components jump across the layer according to [10, eqs. (3) and (4)]

$$E_r^+ - E_r^- = -(R^{\mathrm{M}} + L^{\mathrm{M}}\partial_t)\langle H_\phi\rangle_-^+ + o(\delta) \tag{6}$$

$$H_\phi^+ - H_\phi^- = -(G^{\mathrm{E}} + C^{\mathrm{E}}\partial_t)\langle E_r\rangle_-^+ + o(\delta) \tag{7}$$

for all $r > 0$ and $t > 0$ as $\delta \downarrow 0$, where the coefficients characterizing the EM properties of the combined layer are given by (3) and (4), again. Once the EM fields satisfying the cross-layer conditions are found, the voltage response induced in the receiving short-wire probe $\mathcal{W}^{\mathrm{R}}$ can be approximately found from

$$V^{\mathrm{R}}(t) \simeq -\ell^{\mathrm{R}} E_z(0, -h^{\mathrm{R}}, t) \tag{8}$$

where $\ell^{\mathrm{R}}$ denotes the wire's length and $E_z = E_z(r, z, t)$ is the $z$-component of the eletric-field strength radiated from the transmitting wire $\mathcal{W}^{\mathrm{T}}$.

## IV. Transform-Domain Problem Solution

The problem is tackled with the aid of the CdH technique [9] that combines a one-sided Laplace transformation with the wave slowness Fourier-type representation in the plane parallel to the layer. To show the notation, the integral expressions are given for the vertical component of the electric-field strength. Hence, the Laplace transformation is written as

$$\hat{E}_z(r, z, s) = \int_{t=0}^{\infty} \exp(-st) E_z(r, z, t)\mathrm{d}t \tag{9}$$

with $\{s \in \mathbb{R}; s > 0\}$ and the wave slowness representation has the following form:

$$\hat{E}_z(r, z, s) = (s/2\pi\mathrm{i})^2 \int_{\kappa=-\mathrm{i}\infty}^{\mathrm{i}\infty} \mathrm{d}\kappa \int_{\sigma=-\mathrm{i}\infty}^{\mathrm{i}\infty} \exp[-s(\kappa x + \sigma y)]\tilde{E}_z(\kappa, \sigma, z, s)\mathrm{d}\sigma \tag{10}$$

in which $s$ plays the role of a scaling parameter and $\kappa$ and $\sigma$ are the slowness parameters along the $x$- and $y$-direction, respectively. The complex slowness representations for the induced voltage in the receiving loop and wire are given in the following sections.

### A. Receiving Loop $\mathcal{L}^{\mathrm{R}}$

Making use of (9) and (10) to solve the problem formulated in Section III-A, the voltage response in the $s$-domain can be represented via

$$\hat{V}^{\mathrm{R}}(s) = -\frac{s^4\mu_0\hat{I}^{\mathrm{T}}(s)\mathcal{A}^{\mathrm{T}}\mathcal{A}^{\mathrm{R}}}{4\pi^2}\int_{\kappa=-\mathrm{i}\infty}^{\mathrm{i}\infty}\mathrm{d}\kappa \int_{\sigma=-\mathrm{i}\infty}^{\mathrm{i}\infty}\exp[-s\gamma(\kappa,\sigma)(h^{\mathrm{T}}+h^{\mathrm{R}})]\tilde{T}_{\perp}(\kappa,\sigma,s)\frac{\kappa^2+\sigma^2}{2\gamma(\kappa,\sigma)}\mathrm{d}\sigma \tag{11}$$

where $\mathcal{A}^{\mathrm{T}}$ denotes the transmitting loop's area and $\tilde{T}_{\perp}(\kappa,\sigma,s)$ has the meaning of (transform-domain) transmission coefficient

$$\tilde{T}_{\perp} = \frac{1}{2}\left[\frac{1-\hat{Y}^{\mathrm{E}}(s)/2\tilde{Y}_{\perp}(\kappa,\sigma)}{1+\hat{Y}^{\mathrm{E}}(s)/2\tilde{Y}_{\perp}(\kappa,\sigma)} + \frac{1-\hat{Z}^{\mathrm{M}}(s)\tilde{Y}_{\perp}(\kappa,\sigma)/2}{1+\hat{Z}^{\mathrm{M}}(s)\tilde{Y}_{\perp}(\kappa,\sigma)/2}\right] \tag{12}$$

where [see (3) and (4)]

$$\hat{Y}^{\mathrm{E}}(s) = G^{\mathrm{E}} + sC^{\mathrm{E}} \tag{13}$$

$$\hat{Z}^{\mathrm{M}}(s) = R^{\mathrm{M}} + sL^{\mathrm{M}} \tag{14}$$

denote the equivalent layer's admittance and impedance, respectively. Furthermore, we used $\tilde{Y}_{\perp}(\kappa,\sigma) = \gamma(\kappa,\sigma)/\mu_0$ and

$$\gamma(\kappa,\sigma) = (1/c_0^2 - \kappa^2 - \sigma^2)^{1/2} \text{ with } \mathrm{Re}(\gamma) \geq 0 \tag{15}$$

to denote the vertical slowness parameter. The integral representation of the induced voltage in the $s$-domain (11) has the form that is amenable to analytical solution via the CdH technique. It is finally noted that the (transform-domain) transmission coefficient (12) has the form that is similar to the ones applying to the *TE*-polarized EM fields [10].

### B. Receiving Wire $\mathcal{W}^{\mathrm{R}}$

Employing now (9) and (10) to solve the EM field radiated from $\mathcal{W}^{\mathrm{T}}$ (see Section III-B), the induced voltage across the port of $\mathcal{W}^{\mathrm{R}}$ can be expressed via

$$\hat{V}^{\mathrm{R}}(s) = -\frac{s^2\hat{I}^{\mathrm{T}}(s)\ell^{\mathrm{T}}\ell^{\mathrm{R}}}{4\pi^2\epsilon_0}\int_{\kappa=-\mathrm{i}\infty}^{\mathrm{i}\infty}\mathrm{d}\kappa \int_{\sigma=-\mathrm{i}\infty}^{\mathrm{i}\infty}\exp[-s\gamma(\kappa,\sigma)(h^{\mathrm{T}}+h^{\mathrm{R}})]\tilde{T}_{\parallel}(\kappa,\sigma,s)\frac{\kappa^2+\sigma^2}{2\gamma(\kappa,\sigma)}\mathrm{d}\sigma \tag{16}$$

where $\ell^{\mathrm{T}}$ denotes the length of the transmitting wire and the pertaining transmission coefficient has the following form:

$$\tilde{T}_{\parallel} = \frac{1}{2}\left[\frac{1-\hat{Z}^{\mathrm{M}}(s)\tilde{Y}_{\parallel}(\kappa,\sigma)/2}{1+\hat{Z}^{\mathrm{M}}(s)\tilde{Y}_{\parallel}(\kappa,\sigma)/2} + \frac{1-\hat{Y}^{\mathrm{E}}(s)/2\tilde{Y}_{\parallel}(\kappa,\sigma)}{1+\hat{Y}^{\mathrm{E}}(s)/2\tilde{Y}_{\parallel}(\kappa,\sigma)}\right] \tag{17}$$

where we used $\tilde{Y}_{\parallel}(\kappa,\sigma) = \epsilon_0/\gamma(\kappa,\sigma)$. Again, the integral representation (16) has the form that can be transformed to the TD via the CdH technique. The inverse transform is carried out in the following section.

## V. Space-Time Problem Solution

In this section, the complex slowness integrals (11) and (16) representing the induced voltages in the receiving probes are transformed analytically to the TD. To that end, we shall largely follow the approach pursued in [14].

### A. Receiving Loop $\mathcal{L}^{\mathrm{R}}$

To cast (11) to the form that resembles the Laplace-transform integral, we shall first introduce the polar variables of integration according to

$$\kappa = \lambda\cos(\psi) \tag{18}$$

$$\sigma = \lambda\sin(\psi) \tag{19}$$

for $\{0 \leq \psi < 2\pi\}$ and $\{\mathrm{Re}(\lambda) = 0, 0 \leq \mathrm{Im}(\lambda) < \infty\}$. Under the substitution $\kappa^2+\sigma^2 = \lambda^2$ and $\mathrm{d}\kappa\mathrm{d}\sigma = \lambda\mathrm{d}\lambda\mathrm{d}\psi$, which leads to

$$\hat{V}^{\mathrm{R}}(s) = -\frac{s^4\mu_0\hat{I}^{\mathrm{T}}(s)\mathcal{A}^{\mathrm{T}}\mathcal{A}^{\mathrm{R}}}{2\pi}\int_{\lambda=0}^{\mathrm{i}\infty}\exp[-s\bar{\gamma}(\lambda)(h^{\mathrm{T}}+h^{\mathrm{R}})] \times \bar{T}_{\perp}(\lambda,s)\lambda^3\mathrm{d}\lambda/2\bar{\gamma}(\lambda) \tag{20}$$

where $\bar{\gamma}(\lambda) = (1/c_0^2 - \lambda^2)^{1/2}$ with $\mathrm{Re}[\bar{\gamma}(\lambda)] \geq 0$ and $\bar{T}_{\perp}(\lambda,s)$ follows from (12) upon replacing $\gamma(\kappa,\sigma)$ with $\bar{\gamma}(\lambda)$. In the ensuing step, we substitute

$$\bar{\gamma}(\lambda)(h^{\mathrm{T}}+h^{\mathrm{R}}) = \tau \tag{21}$$

where $\tau$ is the (real-valued and positive) time parameter. Introducing $\tau$ as the new variable of integration, we arrive at

$$\hat{V}^{\mathrm{R}}(s) = -\frac{s^4\mu_0\hat{I}^{\mathrm{T}}(s)\mathcal{A}^{\mathrm{T}}\mathcal{A}^{\mathrm{R}}}{4\pi(h^{\mathrm{T}}+h^{\mathrm{R}})^3}\int_{\tau=T}^{\infty}\exp(-s\tau)\bar{T}_{\perp}[\lambda(\tau),s] \times (\tau^2-T^2)\mathrm{d}\tau \tag{22}$$

where $T = (h^{\mathrm{T}}+h^{\mathrm{R}})/c_0$ is the pulse travel time, which has the form that can be transformed to the TD, in a unique way relying on Lerch's uniqueness theorem [21, Appendix], with the aid of the Schouten-Van der Pol theorem [19, p. 1056]. In this manner, we get

$$V^{\mathrm{R}}(t) = -\frac{\mu_0\mathcal{A}^{\mathrm{T}}\mathcal{A}^{\mathrm{R}}\partial_t^4 I^{\mathrm{T}}(t)}{4\pi(h^{\mathrm{T}}+h^{\mathrm{R}})^3} *_t \int_{\tau=T}^{t} T_{\perp}[\lambda(\tau),t-\tau] \times (\tau^2-T^2)\mathrm{d}\tau \tag{23}$$

for $t > T$, where $T_{\perp}(\lambda,t)$ denotes the TD counterpart of the transmission coefficient $\bar{T}_{\perp}(\lambda,s)$ [see (12)]. A particularly enlightening TD expression can be found for a loss-free combined layer by taking $G^{\mathrm{E}} \downarrow 0$ and $R^{\mathrm{M}} \downarrow 0$, which yields

$$V^{\mathrm{R}}(t) = -V_0^{\mathrm{R}}(t) - \frac{\mu_0\mathcal{A}^{\mathrm{T}}\mathcal{A}^{\mathrm{R}}\partial_t^4 I^{\mathrm{T}}(t)}{4\pi(h^{\mathrm{T}}+h^{\mathrm{R}})^3}$$

$$*_t \int_{\tau=T}^{t} \big\{ \bar{\Psi}_\perp(\tau) \exp[-\bar{\Psi}_\perp(\tau)(t-\tau)] + \bar{\Omega}_\perp(\tau) \exp[-\bar{\Omega}_\perp(\tau)(t-\tau)] \big\} (\tau^2 - T^2) \mathrm{d}\tau \tag{24}$$

for $t > T$, where

$$\bar{\Psi}_\perp(\tau) = (2Y_0/C^{\mathrm{E}})[c_0\tau/(h^{\mathrm{T}} + h^{\mathrm{R}})] \tag{25}$$

$$\bar{\Omega}_\perp(\tau) = (2/Y_0\ L^{\mathrm{M}})[(h^{\mathrm{T}} + h^{\mathrm{R}})/c_0\tau] \tag{26}$$

and

$$V_0^{\mathrm{R}}(t) = -(1/2\pi Y_0) \left[\mathcal{A}^{\mathrm{T}}\mathcal{A}^{\mathrm{R}}/(h^{\mathrm{T}} + h^{\mathrm{R}})^4\right] \times \left[T\partial_t I^{\mathrm{T}}(t-T) + T^2\partial_t^2 I^{\mathrm{T}}(t-T)\right] \tag{27}$$

is the "Thévenin's equivalent voltage generator" pertaining to the pulsed EM signal transfer between two mutually parallel loops located in the unbounded, isotropic, and loss-free medium [20, Sec. IX]. Apparently, $V_0^{\mathrm{R}}(t)$ consists of near- and intermediate-field constituents that are proportional to $(h^{\mathrm{T}} + h^{\mathrm{R}})^{-3}$ and $(h^{\mathrm{T}} + h^{\mathrm{R}})^{-2}$, respectively (see Fig. 1). In the (near-field) limit $T \downarrow 0$, (27) has the form $V_0^{\mathrm{R}}(t) = -L^{\mathrm{c}}\partial_t I^{\mathrm{T}}(t) + O(T)$, where

$$L^{\mathrm{c}} = (\mu_0/2\pi)\mathcal{A}^{\mathrm{T}}\mathcal{A}^{\mathrm{R}}/(h^{\mathrm{T}} + h^{\mathrm{R}})^3 \tag{28}$$

has the meaning of coupling inductance. Such lumped-circuit parameters are frequently applied to initial designs of wireless power transfer systems (e.g., [22]). The TD analytical expression (24) reveals that if both parameters $C^{\mathrm{E}}/Y_0 t_{\mathrm{w}}$ and $L^{\mathrm{M}}Y_0/t_{\mathrm{w}}$ are sufficiently high, then the integral term in (24) tends to zero, which yields $V^{\mathrm{R}}(t) \simeq -V_0^{\mathrm{R}}(t)$. In such a case, the combined layer behaves as a transparent sheet, and the pulsed EM field transmission across the relevant layer merely inverts the pulse's polarity. Physically, the TD phenomenon can be explained in terms of induced electric and magnetic currents whose effects virtually cancel each other, an effect that was evidenced in [10] for 2-D configurations but is now also validated for the 3-D case. The conditions for achieving the EM transparency of a combined sheet for a causal TD EM-field source have been originally put forward in [10].

### B. Receiving Wire $\mathcal{W}^{\mathrm{R}}$

We next pursue the approach from the previous section to transform (16) to the TD. Hence, introducing the polar coordinates $\{\lambda, \psi\}$ in (16) according to (18) and (19), we get an integral representation in the complex plane of the radial slowness parameter $\lambda$ that is subsequently replaced with the purely real-valued $\tau$ [see (21)]. This way leads to [cf. eq. (22)]

$$\hat{V}^{\mathrm{R}}(s) = -\frac{s^2 \hat{I}^{\mathrm{T}}(s)\ell^{\mathrm{T}}\ell^{\mathrm{R}}}{4\pi\epsilon_0(h^{\mathrm{T}} + h^{\mathrm{R}})^3} \int_{\tau=T}^{\infty} \exp(-s\tau)\bar{T}_\parallel[\gamma(\tau), s] \times (\tau^2 - T^2)\mathrm{d}\tau \tag{29}$$

that is transformed to the TD using the Schouten-Van der Pol theorem [19, p. 1056] and we get

$$V^{\mathrm{R}}(t) = -\frac{\ell^{\mathrm{T}}\ell^{\mathrm{R}}\partial_t^2 I^{\mathrm{T}}(t)}{4\pi\epsilon_0(h^{\mathrm{T}} + h^{\mathrm{R}})^3} *_t \int_{\tau=T}^{t} T_\parallel[\lambda(\tau), t-\tau] \times (\tau^2 - T^2)\mathrm{d}\tau \tag{30}$$

for $t > T$, where $T_\parallel(\lambda, t)$ is the TD original of $\bar{T}_\parallel(\lambda, s)$ [see (17)]. Considering now a loss-free combined layer, the TD induced voltage in $\mathcal{W}^{\mathrm{R}}$ can be expressed as

$$V^{\mathrm{R}}(t) = -V_0^{\mathrm{R}}(t) - \frac{\ell^{\mathrm{T}}\ell^{\mathrm{R}}\partial_t^2 I^{\mathrm{T}}(t)}{4\pi\epsilon_0(h^{\mathrm{T}} + h^{\mathrm{R}})^3} *_t \int_{\tau=T}^{t} \big\{ \bar{\Omega}_\parallel(\tau) \exp[-\bar{\Omega}_\parallel(\tau)(t-\tau)] + \bar{\Psi}_\parallel(\tau) \exp[-\bar{\Psi}_\parallel(\tau)(t-\tau)] \big\} (\tau^2 - T^2)\mathrm{d}\tau \tag{31}$$

for $t > T$, where [cf. (25) and (26)]

$$\bar{\Psi}_\parallel(\tau) = (2Y_0/C^{\mathrm{E}})[(h^{\mathrm{T}} + h^{\mathrm{R}})/c_0\tau] \tag{32}$$

$$\bar{\Omega}_\parallel(\tau) = (2/Y_0\ L^{\mathrm{M}})[c_0\tau/(h^{\mathrm{T}} + h^{\mathrm{R}})]. \tag{33}$$

Again, $V_0^{\mathrm{R}}(t)$ denotes the voltage pulse that would be excited in the absence of the combined layer. This response can be readily found in closed form

$$V_0^{\mathrm{R}}(t) = -(1/2\pi Y_0) \left[(\ell^{\mathrm{T}}\ell^{\mathrm{R}})/(h^{\mathrm{T}} + h^{\mathrm{R}})^2\right] \times [T^{-1}\partial_t^{-1} I^{\mathrm{T}}(t-T) + I^{\mathrm{T}}(t-T)]. \tag{34}$$

Likewise (27), (34) is composed of the near- and intermediate-field constituents. On the other hand, as far as the time coordinate is concerned, their properties are very different. In the near-field region, $V_0^{\mathrm{R}}(t) = -\partial_t^{-1} I^{\mathrm{T}}(t)/C^{\mathrm{c}} + O(T)$ as $T \downarrow 0$, where

$$C^{\mathrm{c}} = 2\pi\epsilon_0(h^{\mathrm{T}} + h^{\mathrm{R}})^3/\ell^{\mathrm{T}}\ell^{\mathrm{R}} \tag{35}$$

can be interpreted as the coupling capacitance. Again, it can be deduced from (31) to (33) that if the layer shows high contrasts in both electric permittivity and magnetic permeability, then the layer is virtually transparent. Again, this TD effect can be explained by the cancellation of scattering effects due to equivalent electric and magnetic currents induced in the combined layer.

## VI. Practical Application

### A. Conceptual Benefits

In this section, we shall discuss the introduced TD analytical expressions (24) and (31). First, if both $C^{\mathrm{E}} \downarrow 0$ and $L^{\mathrm{M}} \downarrow 0$ (representing a void layer), then the integral terms tends to $2V_0^{\mathrm{R}}(t)$, which yields $V^{\mathrm{R}}(t) = V_0^{\mathrm{R}}(t)$ in total, as expected. Second, if either $C^{\mathrm{E}} \to \infty$ and $L^{\mathrm{M}} \downarrow 0$ (representing a PEC surface) or $C^{\mathrm{E}} \downarrow 0$ and $L^{\mathrm{M}} \to \infty$ (representing a PMC surface) the integral terms on the right-hand sides of (24) and (31) approach to $V_0^{\mathrm{R}}(t)$, which leads to the zero voltage response induced in the receiving probe below the (perfectly conducting) layer. Third, if both $C^{\mathrm{E}} \to \infty$ and $L^{\mathrm{M}} \to \infty$, the combined layer is effectively transparent, as already discussed in Sections V-A and V-B.

### B. Illustrative Numerical Experiments

The special cases discussed in Section VI-A pertaining the loop-to-loop configuration are next illustrated numerically. To this end, the closed-form TD expression (24) has been implemented in MATLAB. In the examples that follow, the transmitting loop antenna is located at the height $h^{\mathrm{T}} = 16\, r^{\mathrm{T}}$, where

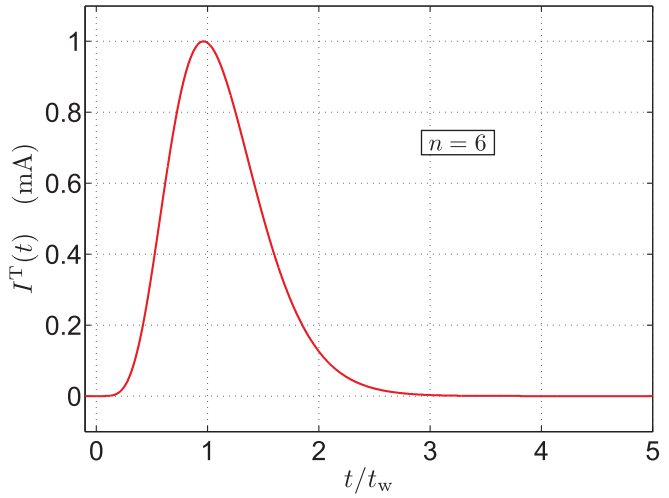


Fig. 2. Excitation electric-current pulse shape.

$r^{\mathrm{T}}$ denotes its radius. The transmitter is excited by the electric-current pulse whose shape is described by [23]

$$I^{\mathrm{T}}(t) = I_{\mathrm{m}}(t/t_{\mathrm{r}})^n \exp[-n(t/t_{\mathrm{r}} - 1)]\mathrm{H}(t) \qquad (36)$$

where we take $I_{\mathrm{m}} = 1.0\,\mathrm{mA}$ and $n = 6$, which implies $t_{\mathrm{r}} \simeq 0.9637\,t_{\mathrm{w}}$. Its pulse time width is related to the distance between the loops via $c_0 t_{\mathrm{w}} = h^{\mathrm{T}} + h^{\mathrm{R}}$. Fig. 2 shows the corresponding exciting pulse shape in the bounded time window $\{0 \le t/t_{\mathrm{w}} \le 5\}$.

The pulsed EM transmitted across the sheet is probed by the receiving loop located at $z = -h^{\mathrm{R}} = -4\,r^{\mathrm{R}}$, where $r^{\mathrm{R}} = r^{\mathrm{T}}$ is the radius of the receiving loop. Consequently, the factor $\mathcal{A}^{\mathrm{T}}\mathcal{A}^{\mathrm{R}}/(h^{\mathrm{T}} + h^{\mathrm{R}})^4 = (\pi/400)^2$ is relatively small [see (27)] and the exciting pulse is relatively wide with respect to the radius of the loops.

First, the electric permittivity and magnetic permeability of the combined sheet are taken to be relatively low such that $C^{\mathrm{E}}/Y_0 t_{\mathrm{w}} = L^{\mathrm{M}} Y_0/t_{\mathrm{w}} = 0.02$. In this case, the voltage response induced in $\mathcal{L}^{\mathrm{R}}$ is (almost) identical to $V_0^{\mathrm{R}}(t)$ applying to the absence of the layer [see Fig. 3(a)]. Second, we consider a highly dielectric layer described by $C^{\mathrm{E}}/Y_0 t_{\mathrm{w}} = 20$ and $L^{\mathrm{M}} Y_0/t_{\mathrm{w}} = 0.02$, which roughly mimics a PEC sheet. Fig. 3(b) demonstrates that the resulting voltage pulse is then strongly attenuated, as expected. Furthermore, we calculate the voltage response in the presence of a sheet showing high contrasts in both electric permittivity and magnetic permeability such that $C^{\mathrm{E}}/Y_0 t_{\mathrm{w}} = L^{\mathrm{M}} Y_0/t_{\mathrm{w}} = 20$. The corresponding induced voltage pulses are shown in Fig. 3(c). It can be seen that the voltage responses are (approximately) inverted copies of each other, thus demonstrating the property of TD EM transparency as predicted in the discussion mentioned above. This observation has a direct practical applicability. The TD analysis clearly demonstrates that thin sheets can become transparent when operated under *causal* pulsed-field conditions. This transparency must be considered in relevant practical scenarios. 1) It can considerably diminish shielding, a subject of interest in, for example, EMC or the construction of radiators using thin sheets as reflectors. 2) The leakage pulses can substantially increase the interference

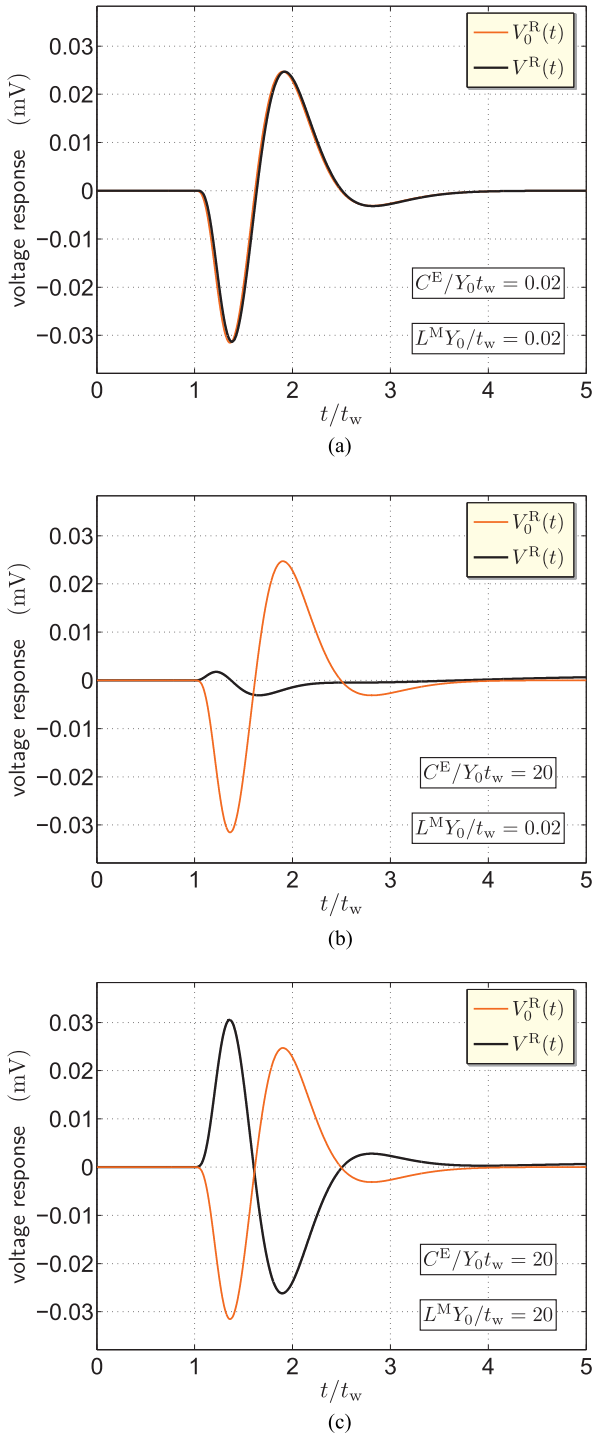


Fig. 3. Computed induced voltage responses in the absence and in the presence of an approximate model of (a) void layer; (b) PEC layer; (c) transparent combined layer.

in highly integrated circuits for ultrafast communications, with possible highly detrimental consequences on the intersymbol interference and, thus, on the bit error rate.

Finally, for validation purposes, we shall evaluate the FD on-axis shielding effectiveness that can be defined via

$$S\mathrm{dB} = 20\log_{10}|\hat{V}_0^{\mathrm{R}}(\mathrm{i}\omega)/\hat{V}^{\mathrm{R}}(\mathrm{i}\omega)| \qquad (37)$$

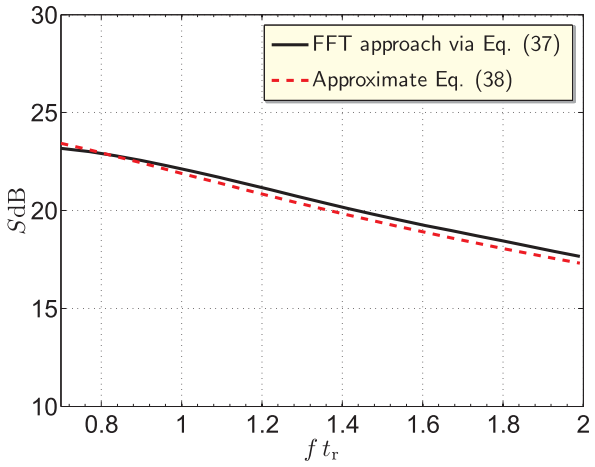


Fig. 4. Shielding factor of a combined sheet described by $C^\mathrm{E}/Y_0 t_\mathrm{w} = 20$ and $L^\mathrm{M} Y_0/t_\mathrm{w} = 0.02$.

where $\omega$ is the (real-valued) angular frequency and $\hat{V}_0^\mathrm{R}(\mathrm{i}\omega)$ with $\hat{V}^\mathrm{R}(\mathrm{i}\omega)$ can be obtained by applying the fast Fourier transform (FFT) to the calculated signals $V_0^\mathrm{R}(t)$ and $V^\mathrm{R}(t)$, respectively. Upon realizing that the FD shielding factor can also be expressed as the ratio of the probed magnetic field in the absence and in the presence of the layer, (37) can be validated with the aid of a straightforward extension of [24, eq. (10.15b)], that is

$$S\mathrm{dB} \simeq 20 \log_{10} \left| \frac{\hat{\Omega}^\mathrm{M}\hat{\Omega}^\mathrm{E} + \hat{\Omega}^\mathrm{M} + \hat{\Omega}^\mathrm{E} + 1}{1 - \hat{\Omega}^\mathrm{M}\hat{\Omega}^\mathrm{E}} \right| \qquad (38)$$

where $\hat{\Omega}^\mathrm{M} = \mathrm{i}\omega L^\mathrm{M} Y_0/2$ and $\hat{\Omega}^\mathrm{E} = \mathrm{i}\omega C^\mathrm{E}/2Y_0$. The shielding factors as calculated for $C^\mathrm{E}/Y_0 t_\mathrm{w} = 20$ and $L^\mathrm{M} Y_0/t_\mathrm{w} = 0.02$ [see Fig. 3(b)] using the FFT-based approach and via (38) are then shown in Fig. 4. As can be seen, a good correlation between the results is achieved, thereby validating the closed-form analytical expressions.

### C. Limitations of the Analytical Model

In order to clearly reveal the principal parameters influencing the physical phenomenon under consideration and to ensure its mathematical tractability, the complexity of a model has to be reduced. Accordingly, the TD analytical expressions introduced in this article were derived under several assumptions that must be properly accounted for in their practical applications. First of all, the use of Laplace transformation (9) entails that the problem configuration is supposed to be time invariant and linear in its EM properties. Consequently, the results are not applicable to calculating the shielding effectiveness of nonlinear and hysteretic shields, for instance, for which dedicated computational approaches have to be used (see [25], for instance). Moreover, as the analyzed sheet is assumed to be of infinite extent, the analytical formulas may not be accurate in applications where edge diffraction effects are critical [26]. Furthermore, the cross-layer conditions (1) with (2) and (6) with (7) have been derived under the assumption that the layer's thickness, $\delta > 0$, is relatively small (with respect to the EM wave speed $\times$ excitation pulse time width) and its magneto-dielectric constitutive parameters, $\{\epsilon, \mu, \sigma, \Gamma\}$, are relatively high (with respect to the ones of the surrounding medium) such that its equivalent layer's Kirchhoff-circuit parameters, $\{G^\mathrm{E}, C^\mathrm{E}, R^\mathrm{M}, L^\mathrm{M}\}$ [see (3) and (4)], are positive constants. Owing to the small (relative) thickness of the layer, multiple reflections inside the slab are not distinguishable and the transmission through the sheet is described by coefficients (12) and (17). This simplification is fully consistent with the concept of first-order (transition) conditions, accuracy of which has been thoroughly discussed in [27, Ch. 2], for instance. The thin-sheet approximation is also frequently employed in quantifying the shielding effectiveness of conductive foils. Indeed, it has been demonstrated in [24, Sec. 10.3.2.3] that the approximation is well applicable to calculating the shielding of highly conducting thin sheets whose thickness is smaller than $1.3 \times$ skin depth. Regarding extremely narrow pulses (with their high-frequency content), the skin depth becomes small while the (relative) thickness of the layer becomes large. In such cases, multiple reflection loss inside the layer cannot be neglected anymore and one has to resort to more accurate models.

## VII. Conclusion

The CdH technique has been applied to develop an analytical TD methodology describing, for the first time, the 3-D on-axis, pulsed EM field signal transfer between two dipole antennas, across a highly contrasting thin sheet with combined magneto-dielectric properties. The arrived at closed-form analytical expressions clearly revealed the possibility of achieving the EM transparency for spatially localized, temporally causal EM sources in a 3-D problem configuration. Illustrative numerical examples validated the conclusions drawn from the analytical results.

## References

[1] NSA 94-106, "Specification for shielded enclosures," *National Security Agency*, 94–106, Oct. 24, 1994.

[2] S. Celozzi and R. Araneo, "Alternative definitions for the time-domain shielding effectiveness of enclosures," *IEEE Trans. Electromagn. Compat.*, vol. 56, no. 2, pp. 482–485, Apr. 2014.

[3] J. H. Kim and C.-H. Ahn, "Method to reduce metal plate effect between transmitter and receiver in wireless power transfer system," *IEEE Antennas Wireless Propag. Lett.*, vol. 17, no. 4, pp. 587–590, Apr. 2018.

[4] S. Cruciani, T. Campi, F. Maradei, and M. Feliziani, "Active shielding design for wireless power transfer systems," *IEEE Trans. Electromagn. Compat.*, vol. 61, no. 6, pp. 1953–1960, Dec. 2019.

[5] P. R. Bannister, "New theoretical expressions for predicting shielding effectiveness for the plane shield case," *IEEE Trans. Electromagn. Compat*, vol. EMC-10, no. 1, pp. 2–7, Mar. 1968.

[6] R. Araneo and S. Celozzi, "Exact solution of the low-frequency coplanar loops shielding configuration," *IEE Proc. - Sci. Meas. Technol.*, vol. 149, no. 1, pp. 37–44, 2002.

[7] G. Lovat, P. Burghignoli, R. Araneo, and S. Celozzi, "Magnetic shielding of planar metallic screens: A new analytical closed-form solution," *IEEE Trans. Electromagn. Compat.*, vol. 62, no. 5, pp. 1884–1888, Oct. 2020.

[8] G. Lovat, P. Burghignoli, R. Araneo, E. Stracqualursi, and S. Celozzi, "Analytical evaluation of the low-frequency magnetic shielding of thin planar magnetic and conductive screens," *IEEE Trans. Electromagn. Compat.*, to be published, doi: 10.1109/TEMC.2020.2989204.

[9] A. T. de Hoop, "A modification of Cagniard's method for solving seismic pulse problems," *Appl. Sci. Res.*, vol. B, no. 8, pp. 349–356, 1960.

[10] M. Štumpf, "Time-domain modeling of thin high-contrast layers with combined dielectric and magnetic properties," *IEEE Antennas Wireless Propag. Lett.*, vol. 19, no. 6, pp. 969–971, Jun. 2020.

[11] A. T. de Hoop and L. Jiang, "Pulsed EM field response of a thin, high-contrast, finely layered structure with dielectric and conductive properties," *IEEE Trans. Antennas Propag.*, vol. 57, no. 8, pp. 2260–2269, Aug. 2009.

[12] A. T. de Hoop, L. L. Meng, and L. J. Jiang, "Pulsed line source response of a thin sheet with high-contrast dielectric and conductive properties—A time-domain analysis," *IEEE Trans. Antennas Propag.*, vol. 61, no. 11, pp. 5649–5657, Nov. 2013.

[13] M. Štumpf and G. A. E. Vandenbosch, "Impulsive electromagnetic response of thin plasmonic metal sheets," *Radio Sci.*, vol. 49, no. 8, pp. 689–697, 2014.

[14] M. Štumpf and A. T. de Hoop, "Loop-to-loop pulsed electromagnetic signal transfer across a thin metal screen with drude-type dispersive behavior," *IEEE Trans. Electromagn. Compat.*, vol. 60, no. 4, pp. 885–889, Aug. 2018.

[15] P. Burghignoli, G. Lovat, R. Araneo, and S. Celozzi, "Time-domain shielding of a thin conductive sheet in the presence of pulsed vertical dipoles," *IEEE Trans. Electromagn. Compat.*, vol. 60, no. 1, pp. 157–165, Feb. 2017.

[16] P. Burghignoli, G. Lovat, R. Araneo, and S. Celozzi, "Pulsed vertical dipole response of a thin sheet with high-contrast dielectric and conductive properties," *IEEE Trans. Antennas Propag.*, vol. 66, no. 1, pp. 217–225, Jan. 2018.

[17] G. Lovat, R. Araneo, P. Burghignoli, and S. Celozzi, "The electromagnetic effects of pulsed horizontal dipoles on a thin conductive sheet: Time-domain analysis," *IEEE Trans. Electromagn. Compat.*, vol. 62, no. 2, pp. 443–450, Apr. 2020.

[18] A. Neto, N. Llombart, J. J. Baselmans, A. Baryshev, and S. J. Yates, "Demonstration of the leaky lens antenna at submillimeter wavelengths," *IEEE Trans. Terahertz Sci. Technol.*, vol. 4, no. 1, pp. 26–32, Jan. 2014.

[19] A. T. de Hoop, *Handbook of Radiation and Scattering of Waves*. London, U.K.: Academic, 1995.

[20] A. T. de Hoop, I. E. Lager, and V. Tomassetti, "The pulsed-field multiport antenna system reciprocity relation and its applications—A time-domain approach," *IEEE Trans. Antennas Propag.*, vol. 57, no. 3, pp. 594–605, Mar. 2009.

[21] M. Štumpf, *Electromagnetic Reciprocity in Antenna Theory*. Hoboken, NJ, USA: Wiley, 2018.

[22] J. Kim *et al.*, "Coil design and shielding methods for a magnetic resonant wireless power transfer system," *Proc. IEEE*, vol. 101, no. 6, pp. 1332–1342, Jun. 2013.

[23] I. E. Lager, A. T. de Hoop, and T. Kikkawa, "Model pulses for performance prediction of digital microelectronic systems," *IEEE Trans. Compon., Packag., Manuf. Technol.*, vol. 2, no. 11, pp. 1859–1870, Nov. 2012.

[24] F. M. Tesche, M. V. Ianoz, and T. Karlsson, *EMC Analysis Methods and Computational Models*. New York, NY, USA: Wiley, 1997.

[25] P. Sergeant, L. Dupré, L. Vandenbossche, and J. Melkebeek, "Analytical formulation for magnetic shields taking into account hysteresis effects in the rayleigh region," *Int. J. Comput. Math. Elect. Electron. Eng.*, vol. 24, no. 4, pp. 1470–1491, 2005.

[26] R. G. Olsen and P. Moreno, "Some observations about shielding extremely low-frequency magnetic fields by finite width shields," *IEEE Trans. Electromagn. Compat.*, vol. 38, no. 3, pp. 460–468, Aug. 1996.

[27] T. B. Senior and J. L. Volakis, *Approximate Boundary Conditions in Electromagnetics*. London, U.K.: The Institution of Electrical Engineers, 1995.


**Martin Štumpf** (Senior Member, IEEE) received the Ph.D. degree in electrical engineering from the Brno University of Technology (BUT), Brno, The Czech Republic, in 2011.

After his Ph.D. research, he spent a year and a half as a Postdoctoral Fellow with the ESAT-TELEMIC Division, Katholieke Universiteit Leuven, Leuven, Belgium. He is currently an Associate Professor with the Department of Radioelectronics, BUT. During a three-month period in 2018, he was a Visiting Professor with the UAq EMC Laboratory, University of L'Aquila, L'Aquila, Italy. He has authored the books *Electromagnetic Reciprocity in Antenna Theory* (Wiley–IEEE Press, 2017), *Pulsed EM Field Computation in Planar Circuits: The Contour Integral Method* (CRC Press, 2018), and *Time-Domain Electromagnetic Reciprocity in Antenna Modeling* (Wiley–IEEE Press, 2019). His main research interests include modeling of electromagnetic wave phenomena with an emphasis on EMC and antenna engineering.

**Giulio Antonini** (Senior Member, IEEE) received the Laurea degree (*cum laude*) in electrical engineering from the University of L'Aquila, L'Aquila, Italy, in 1994 and the Ph.D. degree in electrical engineering from the University of Rome "La Sapienza," Rome, Italy, in 1998.

Since 1998, he has been with the UAq EMC Laboratory, University of L'Aquila, where he is currently a Professor. He has coauthored the book *Circuit Oriented Electromagnetic Modeling Using the PEEC Techniques*, (Wiley–IEEE Press, 2017). His scientific research interests are in the field of computational electromagnetics.

**Ioan E. Lager** (Senior Member, IEEE) received the M.Sc. degree in electrical engineering from the "Transilvania" University of Braşov, Braşov, Romania, in 1987, the Ph.D. degree in electrical engineering from Delft University of Technology, Delft, The Netherlands, in 1996, and the second Ph.D. degree in electrical engineering from the "Transilvania" University of Braşov, Braşov, Romania, in 1998.

He successively occupied several research and academic positions with the "Transilvania" University of Braşov and the Delft University of Technology, where he is currently an Associate Professor. In 1997, he was a Visiting Scientist with Schlumberger-Doll Research, Ridgefield, CT, USA. He has a special interest for bridging the gap between electromagnetic field theory and the design, implementation and physical measurement of radio-frequency front-end architectures. His research interests are in applied electromagnetics, especially time-domain propagation and applications, and antenna engineering, with an emphasis on nonperiodic (interleaved) array antenna architectures. He currently investigates effective methods for teaching electromagnetic field theory at (under)graduate-level.

**Guy A. E. Vandenbosch** (Fellow, IEEE) received the M.S. and Ph.D. degrees in electrical engineering from the Katholieke Universiteit Leuven, Leuven, Belgium, in 1985 and 1991, respectively.

From 1991 to 1993, he held a Postdoctoral Research position with the Katholieke Universiteit Leuven, where he has been a Lecturer, since 1993, and a Full Professor, since 2005. He has taught or teaches courses on "Electromagnetic Waves," "Antennas," "Electromagnetic Compatibility," "Electrical Engineering, Electronics, and Electrical Energy," and "Digital Steer- and Measuring Techniques in Physics." From September to December 2014, he was a Visiting Professor with the Tsinghua University, Beijing, China. His research interests are in the area of electromagnetic theory, computational electromagnetics, planar antennas and circuits, nano-electromagnetics, EM radiation, EMC, and bioelectromagnetics. His work has been authored or coauthored in ca. 310 papers in international journals and has led to ca. 375 papers at international conferences.

Dr. Vandenbosch has been a member of the "Management Committees" of the consecutive European COST actions on antennas since 1993. Within the ACE Network of Excellence of the EU (2004–2007), he was a member of the Executive Board and coordinated the activity on the creation of a European antenna software platform. At present, he leads the EuRAAP Working Group on Software and represents this group within the EuRAAP Delegate Assembly. From 2001 to 2007, he was the President of SITEL, the Belgian Society of Engineers in Telecommunication and Electronics. From 2008 to 2014, he was a member of the board of FITCE Belgium, the Belgian branch of the Federation of Telecommunications Engineers of the European Union. In the period 1999–2004, he was the Vice-Chairman, in the period 2005–2009, a Secretary, and in the period 2010–2017, the Chairman of the IEEE Benelux Chapter on Antennas and Propagation. In the period 2002–2004, he was a Secretary of the IEEE Benelux Chapter on EMC. In the period 2012–2014, he was a Secretary of the Belgian National Committee for Radio-electricity (URSI), where he is also in Charge of Commission E.